Surface fibrils of *Streptococcus oralis* subsp. *dentisani*

Research Thesis

Presented in partial fulfillment of the requirements for graduation with research distinction in the undergraduate colleges of The Ohio State University

by

Allen Ronis

The Ohio State University

April 2019

Project Advisor: Dr. Samantha J. King, College of Medicine

ABSTRACT

Streptococcus oralis is an oral commensal bacterium and a leading cause of sub-acute infective endocarditis (IE). Little is known of the mechanisms by which this bacterium colonizes the oral cavity and causes sub-acute IE. A crucial step in both processes is adhesion to host surfaces, yet no adhesion mechanisms have been defined for *S. oralis* subsp. *dentisani*. Electron microscopy images of *S. oralis* subsp. *dentisani* endocarditis isolates identified dense mono-lateral fibrils. Other streptococcal species have been shown to bind oral and IE relevant host surfaces, including oral epithelial cells, saliva and platelets, via serine-rich repeat proteins (SRRPs), a family of bacterial adhesins which typically form fine fibrils evenly distributed over the bacterial surface. However, *S. cristatus* has dense mono-lateral fibrils associated with an SRRP. This led to the hypothesis that *S. oralis* subsp. *dentisani* encodes one or more SRRPs that produce mono-lateral fibrils and act as adhesins. Analysis of a genome sequenced *S. oralis* subsp. *dentisani* isolate revealed three genes encoding putative SRRPs. A panel of SRRP mutants was generated and showed that each putative SRRP locus produces mono-lateral fibrils. The secondary structures of SRRPs are composed of two serine-repeat regions flanking a non-repeat region (NRR). Receptors for members of the SRRP family differ based on domains within the NRR. Structural predictions of the NRR suggest that two of these SRRPs, FapA and FapB, play a role in biofilm formation and intra- and interspecies interactions. Initial experiments suggest that FapA and FapB contribute to the auto-aggregation of this isolate. The FapC NRR contains predicted domains previously shown to bind sialic acid in other SRRPs. FapC mutants showed a significant reduction in adherence to saliva, which is heavily sialylated, suggesting FapC is required for efficient binding to sialic acid. FapC is the first adhesin described for *S. oralis* subsp. *dentisani*.

ACKNOWLEDGEMENTS

I would like to thank all who have been mentors to me throughout this process and made this thesis possible. First, Dr. Samantha King, who has been the most supportive and devoted mentor I could have asked for as an undergraduate. Dr. Anirudh Singh, for his direction and wisdom both inside and outside of the lab. Dr. Meztlli Gaytan, for giving me much appreciated help and guidance in experiments. Dr. Jane Jackman, for being a guide to me in the classroom and taking the time to hear my thesis defense. Finally, my friends and family, for their unconditional support and understanding in the importance of this project to me.

CONTENTS

Abstract ..... **i**

Introduction **1**

Methods **4**

Table 1: Strains used in this study **11**

Table 2: Primers used in this study **13**

Results **16**

Figure 1: *S. oralis* subsp. *dentisani* electron microscopy **16**

Figure 2: Schematic of loci encoding putative SRRPs **17**

Figure 3: F0392 mutant panel **19**

Figure 4: Putative domains within SRRP non-repeat regions of F0392 ..... **20**

Figure 5: Adherence of F0392 to saliva **22**

Figure 6: rFapC$_{217-938}$ blocking assay **23**

Figure 7: Adherence of F0392 to neuraminidase treated saliva **24**

Figure 8: Sialic acid blocking assay **25**

Figure 9: Auto-aggregation of F0392 wild-type and mutant strains **26**

Discussion **26**

INTRODUCTION

Infective endocarditis (IE) is responsible for one in every thousand hospital admissions in the United States (1). An infection of the heart endocardium, IE is a particularly devastating disease, resulting in a 10% mortality rate in-hospital and a 40% mortality rate a year post diagnosis (2). Although IE is clearly a large health concern in the U.S., the incidence of IE has not decreased in the past 30 years (2). Therefore, it is critical that we better understand the factors and pathways by which IE manifests, so we may better design and implement new preventative and therapeutic strategies.

Infective endocarditis is split into two types, each characterized by their pathogenesis. Acute IE frequently occurs in intravenous drug users and is characterized by a rapid onset (1). No pre-existing heart valve damage is necessary in the pathogenesis of acute IE. Alternatively, sub-acute IE requires pre-existing heart valve damage before infection can occur. Blood-borne bacteria may then adhere to this damage and form a nidus. Over time, a vegetation may begin to grow, impeding proper heart function and posing the potential of breaking off and causing a stroke (3). Symptoms of sub-acute IE include fever, night sweats, and weight loss (4). Because symptoms are largely non-specific, sub-acute IE can go undetected for long periods of time, making it particularly difficult to treat those afflicted as the infection has grown over time. As IE is most prevalent in elderly populations, rates of IE will increase as our population ages, making it important we find alternative methods of detection and treatment now (5).

Subacute IE is frequently caused by Viridans group streptococci, of which *Streptococcus oralis* is a member (4). *Streptococcus oralis* is an oral commensal and a leading cause of subacute IE (6, 7). Improvements in genomics, such as multilocus sequence analysis, has led to the addition of *Streptococcus dentisani, Streptococcus mitis* biovar 2, and *Streptococcus tigurinus* to the *S.*

oralis taxon, which was then divided into three subspecies: *S. oralis* subsp. *oralis*, *S. oralis* subsp. *tigurinis* and *S. oralis* subsp. *dentisani* (8, 9). All three of these subspecies have been isolated from the blood of IE patients (6, 10-12). Adhesion to host surfaces and receptors is critical in both the oral cavity during colonization and the heart endocardium during IE. Although this bacterium is a primary cause of subacute IE, very little is known of the mechanisms by which it adheres to host surfaces during colonization or IE. It is therefore critical we gain an understanding of the methods and mechanisms by which these bacteria bind to host surfaces, so we may identify prominent drug targets and potential therapeutic treatments.

Serine-rich repeat proteins (SRRPs) are a family of bacterial adhesins which can mediate binding to several host and bacterial surfaces in pathogenic and commensal Gram-positive organisms (13-18). SRRPs are named for their two heavily glycosylated serine-rich repeats (SRRs) which flank a non-repeat region (NRR). All defined SRRP-receptor interactions identified thus far have been shown to be facilitated through the modular NRR, located within the N-terminal region of the protein (14). Previously identified receptors include sialic acid, keratins, fibrinogen, DNA, rhamnogalacturonan I, polygalacturonic acid and chondroitin sulfate (14-16, 19-21). Most SRRPs are characterized to bind a single receptor, however, pneumococcal SRRP PsrP has been shown to bind multiple receptors (20-22).

Bacterial SRRPs have also been implicated in inter- and intraspecies interactions. *Streptococcus cristatus* SRRP SrpA has been shown to be required for binding to *Fusobacterium nucleatum* and *Corynebacterium matruchotti in vitro* (23-25). It has also been reported that pneumococcal SRRP PsrP plays a role in intraspecies interactions which promote bacterial aggregation in the nasopharynx and lungs of infected mice, as well as in models of mature biofilms (26).

Additionally, *Staphylococcus aureus* SRRP SraP and *Streptococcus gordonii* SRRP GspB were shown to be involved in intraspecies bacterial adhesion by promoting bacterial aggregation (26).

In all SRRPs described, a single genomic region encodes for the SRRP(s) and proteins required for glycosylation (GftA/B) and secretion (SecA2/Y2) of the SRRP (14, 27, 28). The cytosolic *O*-glycosyltransferase, GftA/B, is a complex of GftA and GftB subunits. GftA/B glycosylates serine and threonine residues of translated SRRP precursors, which is necessary for stability of the SRRP (14, 29). The SecA2/Y2 system is proposed to be dedicated to the secretion of SRRPs (27). The SRRP is targeted to the accessory secretion system via an atypical N-terminal 90 amino acid secretion signal. Different streptococcal species, and even in some cases different strains, encode unique SRRPs. Most streptococcal species encode for and produce a single SRRP, although there have been cases of streptococcal species encoding for multiple SRRPs, such as *Streptococcus salivarius*, which was found to encode for three SRRPs (13). Additionally, some strains of *Lactobacillus* have been reported to encode for multiple SRRPs (30).

Although the structure and appearance of SRRPs has received limited investigation, SRRPs are typically associated with thin fibrils that are evenly distributed across of the bacterial surface (13, 14, 28, 31-33). Some deviations exist, including *Streptococcus cristatus*, which has been reported to produce mono-lateral, or one-sided, tufts made up of fibrils of two lengths, long and short (23, 25, 34). A variant of this strain lacking the 5' end of the gene encoding for the SRRP SrpA no longer displayed the longer of the two fibrils, linking this SRRP with the production of the long fibrils (23, 35, 36).

Streptococcus oralis subsp. *oralis* IE isolates have previously been reported to encode for SRRP Fap1, which was found to be required for binding to both terminal sialic acid and cryptic β-1,4 linked galactose revealed by *S. oralis* neuraminidase (17). However, *fap1* is not present in *S.*

oralis subsp. *dentisani* isolate F0392, meaning adhesion of this isolate to host surfaces must be facilitated via a distinct SRRP or an SRRP-independent mechanism.

The primary goal of this study was to identify and characterize the dense mono-lateral fibrils imaged on *S. oralis* subsp. *dentisani* isolate F0392. Because of its similarity in appearance to the SRRP expressing *S. cristatus*, the presence of multiple SRRP encoding open-reading frames in the F0392 genome and the fact that all identified functions of SRRPs have centered around bacterial adhesion, we hypothesized that *S. oralis* subsp. *dentisani* isolate F0392 encodes for multiple SRRPs which produce mono-lateral fibrils and act as adhesins. As *S. oralis* is a primary cause of sub-acute IE, we hope study of the adhesins of this organism may yield invaluable data leading to a greater insight of the mechanisms by which this bacterium colonizes the oral cavity and causes sub-acute IE. Knowledge of these mechanisms will likely identify new drug targets in IE pathogenesis and ultimately ease the burden of IE.

METHODS

Bacterial strains, culture, media, and chemicals

Wild-type and genetically altered strains of *S. oralis* subsp. *dentisani* are listed in Table 1. *S. oralis* subsp. *dentisani* was grown overnight at 37 ^{o}C and 5% CO_2 on tryptic soy agar plates supplemented with 5% sheep's blood (Becton, Dickinson and Co., Sparks, MD) or tryptic soy (TS) agar plates spread with 5000 U catalase (Worthington Biochemical Corporation, Lakewood, NJ) prior to plating. Broth cultures were grown statically in Todd-Hewitt broth (Becton, Dickinson and Co.) supplemented with 0.2% w/v yeast extract (Becton, Dickinson and Co.) (THY). C + Y media with 5% yeast extract (C+Y) pH 8.0 was used for transformations (37). Mutant *S. oralis* strains were selected on TS agar plates supplemented with spectinomycin (200

μg/mL), erythromycin (1 μg/mL), kanamycin (500 μg/mL), streptomycin (200 μg/mL) or chloramphenicol (2.5 μg/mL) as appropriate.

Escherichia coli were grown at 120 rpm in Luria-Bertani (LB) broth or LB agar plates. *E. coli* containing cloned plasmids were selected using media supplemented with spectinomycin (50 μg/mL), erythromycin (200 μg/mL), kanamycin (50 μg/mL), chloramphenicol (30 μg/mL) or ampicillin (100 μg/mL) as appropriate (Thermo Fisher Scientific).

Unless otherwise specified, all chemicals, substrates, and enzymes were purchased from Sigma-Aldrich (St. Louis, MO).

Genomic DNA Prep

S. oralis subsp. *dentisani* wild-type and mutant DNA was isolated by first growing strains in THY to OD_{600} = 0.6 and harvesting cells by centrifugation at 4000 rpm for 10 minutes. Bacterial cells were then washed and resuspended in 500 μL of resuspension buffer (50 mM NaCl, 10 mM Tris-HCl, pH 7.4). 15 μL of mutanolysin was added and the mixture was incubated overnight in a 37 °C water bath. 10 μL of EDTA (0.5 M) was added followed by incubation at 37 °C for 30 minutes. Proteinase K was added to a final concentration of 100 μg/mL and the mixture was incubated at 55 °C for 10 minutes. Subsequently, 40 μL of 20% N-lauryl sarcosine was added followed by a 10-minute incubation period. Samples were then subjected to two rounds of extraction with an equal volume of phenol:chloroform:isoamyl alcohol and a final extraction with an equal volume of chloroform. DNA was precipitated upon addition of 0.7 volumes of cold isopropanol. The pellet was washed twice with 70% ethanol, air-dried, and resuspended in 50 μL dH_2O.

Microscopy and Staining

S. oralis subsp. *dentisani* strains were imaged using a Hitachi S-4800 scanning electron microscope in scanning transmission mode (STEM) with a bottom-mounted electrodetector or a Hitachi H-7650 transmission microscope with a CCD detector (Hitachi High Technologies America, Schaumburg, IL). Strains were grown to $OD_{600} = 0.3 \pm 0.005$, after which bacteria were bound to formvar coated grids stabilized with evaporated carbon film (EMS, Hatfield, PA). Grids were washed three times in water and negatively stained with 1% ammonium molybdate.

Mutant Generation

Insertion-deletion mutants were generated via allelic exchange. SecA2 mutants were generated by first amplifying fragments upstream and downstream of *secA2* using primers E.i with E.ii and E.iii with E.iv respectively. A spectinomycin cassette was amplified using primers S.F. and S.R. These fragments were cloned into EcoRI-digested pDrive (Qiagen) via the In-Fusion EcoDry HD cloning kit (Clontech, Mountain View, CA) and transformed into *E. coli* Stellar competent cells (Clontech). Transformants were selected for on LB agar plates supplemented with spectinomycin. Constructs were confirmed via colony PCR using M13F and T7 promoter primers and sequencing. *S. oralis* subsp. *dentisani* was subsequently transformed by growing bacteria in C+Y media to $OD_{600} = 0.12\text{-}0.2$ followed by addition of 50 µL of culture to a transformation mixture containing 950 µL C+Y, 10 µL $CaCl_2$ (100 mM), 2 µL competency-stimulating peptide (1 mg/mL) and about 100 ng of purified plasmid. This mix was incubated in a 37 ^{o}C water bath for two hours and transformants were selected for on TS agar plates supplemented with spectinomycin. Mutants were confirmed using primers flanking the construct (E.5 and E.6).

Serine-rich repeat protein (SRRP) mutant constructs were generated via an inverse PCR method. A fragment of each SRRP encoding gene was amplified using respective primer pairs (1 and 2),

and subsequently cloned into pJet1.2/Blunt PCR cloning vector (Thermo Fisher Scientific) and transformed into *E. coli* Stellar via In-fusion cloning. Transformants were selected on LB agar plates supplemented with ampicillin and confirmed via PCR. Successfully cloned plasmids were isolated and an inverse PCR product was generated with primers 3 and 4. The inverse PCR product was then blunt end ligated to either a spectinomycin, erythromycin or kanamycin antibiotic resistance cassette, cloned into *E. coli* Stellar and plated on LB agar plates supplemented with appropriate antibiotics. Final plasmid constructs were confirmed via PCR. The plasmid was subsequently transformed into *S. oralis* subsp. *dentisani* following the transformation protocol outlined above. Mutants were confirmed to contain the antibiotic cassette and thus the mutation by PCR using primers flanking the construct (5 and 6) and checking that the size of this PCR product was consistent with the size of the inserted fragment.

F0392 point mutants were generated using the two-step Janus cassette system (38). Two overlapping fragments were amplified using primers which introduced the appropriate codon change (Primers 11 and 12, 13 and 14). The two fragments were then joined together via splicing by overlap (SOE) PCR using primers 11 and 14. This fragment was then cloned into pGex-5X-3 via In-Fusion cloning and transformed into *E. coli* Stellar, generating the point mutant plasmid construct pGex-5X-3 FapCR837E. Transformants were selected on LB agar plates supplemented with ampicillin and constructs were confirmed via PCR and sequencing. To generate the Janus intermediate cassette (pGex-5x-3 FapC Janus), an inverse PCR product was produced using primers 15 and 16 and pGex-5X-3 FapCR837E as a template. The inverse PCR product was then blunt-end ligated to a Janus cassette (primers J.F and J.R), followed by cloning into *E. coli* Stellar and selection on LB agar plates supplemented with kanamycin. The construct was confirmed via PCR. Because the Janus cassette imparts streptomycin sensitivity, a streptomycin

resistant strain of *S. oralis* subsp. *dentisani* (F0392 Sm^r) is necessary for selection. F0392 Sm^r was generated by transformation with an *rpsL* PCR product from an Sm^r *S. oralis* strain and selected for on TS agar plates supplemented with streptomycin (primers R.F and R.R). F0392 Sm^r was then transformed using pGex-5X-3 FapC Janus, yielding a Janus intermediate strain. Transformants were selected for on TS agar plates supplemented with kanamycin. Mutants were confirmed by PCR using primers 11 and 14. A subsequent transformation with pGex-5X-3 FapCR837E replaced the Janus cassette with an unmarked sequence containing the arginine to glutamic acid point mutation. Transformants were selected for on TS agar plates supplemented with streptomycin and verified via PCR (Primers 11 and 14) and sequencing.

The genetic background of all mutants was confirmed by extragenic palindromic PCR (REP PCR) (39). All mutants were confirmed to be absent of generalized growth defects by analyzing growth on rich medium. Another member of our lab also checked mutants for polarity via RT-PCR of downstream genes.

Expression and purification of recombinant $FapC_{217-938}$

The NRR of *fapC*, encoding amino acids 217-938, was amplified using primers C.18 and C.19. This fragment was then cloned into GST-tagged pGex-5X-3 via In-Fusion cloning, followed by transformation into *E. coli* Stellar and selection on LB agar plates supplemented with ampicillin. The expression construct was confirmed by PCR and sequencing. BL21 (DE3) competent *E. coli* (New England Biolabs, Ipswich, MA) were transformed using this construct. Transformants were selected for on LB agar plates supplemented with ampicillin. Cultures were inoculated in LB broth and grown at 37 °C to OD_{600} = 0.6-0.8. Expression was induced by the addition of 0.5 mM IPTG. The induced culture was incubated overnight at 120 RPM, 22 °C. Cells were harvested by centrifugation at 5000 RPM and 4 °C for 15 minutes and resuspended in 1/10 the

original volume in PBS. Cells were lysed using a French Press at 24 kPa. Cell debris was collected by centrifugation at 10,000 rpm and 4 °C for 15 minutes and the supernatant was separated from the cell debris. Resuspended cell debris and supernatant were run on an SDS-PAGE gel to ensure that the protein was produced and soluble. Soluble protein in the supernatant was purified via affinity chromatography using Glutathione Sepharose 4B GST-tagged protein purification resin (GE Healthcare Life Sciences, Marlborough, MA), followed by elution with 50 mM tris-HCl, 10 mM glutathione and dialysis against PBS, yielding concentrated $rFapC_{217-938}$. Purified protein was verified via SDS-PAGE for correct size and purity. Purified protein was quantified by measuring absorbance at 280 nm.

Saliva Binding Assays

Saliva (Lee Biosciences, Maryland Heights, Mo) was clarified by centrifugation of 1.2 mL of whole saliva at 21,000 g at 4 °C for 20 minutes. The supernatant was separated and filter sterilized. Assays were conducted in 96-well plates. To coat plates, saliva was diluted 5X in PBS and 100 µL of diluted saliva was used per well. Plates were left at 4 °C overnight and then washed twice with 120 µL PBS to remove non-adherent saliva. Bacterial cultures were grown to $OD_{600} = 0.300 \pm 0.005$ and diluted 25X in PBS. 50 µL of diluted bacterial culture was added per well followed by incubation at 37 °C for one hour. Non-adherent bacteria were removed by washing three times with 120 µL PBS. Adherent bacteria were lifted with 100 µL of 0.25% trypsin/1 mM EDTA at 37 °C for fifteen minutes. Bacteria were enumerated by serial dilution from 10^0 to 10^{-3} and plating. All binding assays were performed three times in triplicate. Significance was determined via a two-tailed student's *t* test, with a P value ≤ 0.05 considered significant.

For experiments involving neuraminidase treated saliva, saliva was diluted 5X in PBS followed by addition of *Clostridium perfringens* neuraminidase to a concentration of 0.1 U/mL. Saliva was neuraminidase treated for 14-16 hours in a 37 °C water bath, followed by coating according to the protocol outlined above. Where appropriate, binding assays were performed in the presence of recombinant FapC non-repeat region ($rFapC_{217-938}$) at a final concentration of 5-7 μM or 1 mM free N-acetylneuraminic acid.

Auto-aggregation Assays

S. oralis subsp. *dentisani* strains were grown in THY to $OD_{600} = 0.600 \pm 0.005$ and cells were harvested by centrifugation at 5000 rpm at 4 °C for 15 minutes. Cells were washed using 0.15 M NaCl twice and resuspended in 0.15 M NaCl to 1/10 of the original volume. 250 μL of the bacterial suspension was added to 1.75 mL of 0.15 M NaCl in a 250 mL Erlenmeyer flask and subsequently shaken at 200 rpm at 37 °C for 2 hours. OD_{600} was measured directly following incubation. Aggregation assays were performed three times. Significance was determined via a two-tailed student's *t* test, with a P value ≤ 0.05 considered significant.

Table 1: Strains used in this study

Strain or plasmid	Characteristic(s)/genotype[a]	Source or reference
Strain		
S. oralis* subsp. *dentisani		
F0392	Originally identified as *Streptococcus mitis* isolated from the human oral cavity	BEI resources[b]
F0392 Δ*secA2*	Δ*secA2*::*aad9*, Spc^r	This study
F0392 Δ*fapA*	Δ*fapA::erm*, Erm^r	This study
F0392 Δ*fapB*	Δ*fapB::kan*, Kan^r	This study
F0392 Δ*fapC*	Δ*fapC*::*aad9*, Spc^r	This study
F0392 Δ*fapB* Δ*fapA*	Δ*fapB::kan* Δ*fapA::erm*, Kan^r Erm^r	This study
F0392 Δ*fapC* Δ*fapA*	Δ*fapC*::*aad9* Δ*fapA::erm*, Spc^r Erm^r	This study
F0392 Δ*fapC* Δ*fapB*	Δ*fapC*::*aad9* Δ*fapB::kan*, Spc^r Kan^r	This study
F0392 Δ*fapC* Δ*fabB* Δ*fapA*	Δ*fapC*::*aad9* Δ*fapB::kan* Δ*fapA::erm*, Spc^r Kan^r Erm^r	This study
F0392 Sm^r	Lys56 → Thr mutation in RpsL [*rpsL*(*K56T*)] conferring Sm^r	This study
F0392 FapC R837E Janus	Δ*fapC*::*kan*/*rpsL*$^+$ *rpsL(K56T)*, Kan^r Sm^s	This study
F0392 FapC R837E	Arg → Glu mutation in FapC [*fapC*(*R837E*)]; *rpsL*(*K56T*) Sm^r	This study
F0392 FapC R837M	Arg → Met mutation in FapC [*fapC*(*R837M*)]; *rpsL*(*K56T*) Sm^r	This study
Escherichia coli		
Stellar	Cloning Host	Takara
BL21 (DE3)	Expression Host	NEB
Plasmids		
pDrive	Cloning vector; Amp^r Kan^r	Qiagen
pDriveΔ*secA2*	pDriveΔ*secA2*::*aad9* Spc^r Amp^r Kan^r	This study
pJET1.2/blunt	Cloning vector; Amp^r	Thermo Fisher Scientific
pJETΔ*fapA*	pJetΔ*fapA*::*erm*, Erm^r Amp^r	This study
pJETΔ*fapB*	pJetΔ*fapB*::*kan*, Kan^r Amp^r	This study
pJETΔ*fapC*	pJetΔ*fapC*::*aad9*, Spc^r Amp^r	This study
pGex-5x-3	Expression vector; Amp^r	GE Biosciences
pGex-5x-3 FapC Janus	pGex-5x-3 FapCR837E with Janus cassette; Amp^r, Kan^r	This study
pGex-5x-3 FapCR837E	pGex-5x-3 containing *fapC* 722-938 with Arg → Glu mutation in FapC [*fapC* (*R837E*)]; Amp^r	This study
pGex-5x-3 FapCR837M	pGex-5x-3 containing *fapC* 722-938 with Arg → Met mutation in FapC [*fapC* (*R837M*)]; Amp^r	This study

pGex-5x-3 FapC$_{217-938}$	pGex-5X-3 containing *FapC* 217-938; Amp^r	This study

[a] Spc^r, spectinomycin resistant; Kan^r, kanamycin resistant; Erm^r, erythromycin resistant, Amp^r, ampicillin resistant; Sm^r, streptomycin resistant.

[b] Strain F0392, HM-262 was obtained through BEI Resources, NIAID, NIH as part of the Human Microbiome Project.

Table 2: Primers used in this study

Target or Group	Name	Sequence 5' to 3'	Location (accession no.)
secA2	E.i	TCGGATCCAGAATTCTCAGATTGCAGAAATGAGAAC[a]	944658-944678 (CP034442)
	E.ii	CACGAACGAAAATCGATCTGGATCATAGGCATTCTG[b]	944102-944122 (CP034442)
	E.iii	ATAAACCCTTGCATAATTCATTTGACCTCTCGTCG[b]	943218-943237 (CP034442)
	E.iv	CTTGTCGACGAATTCAACAGTCATCTATCGCTCTC[a]	942780-942800 (CP034442)
	E.5	ACTAAACGATTCAATTTGAC	944931-944950 (CP034442)
	E.6	TAATGTAACTCAATGCCATG	942610-942629 (CP034442)
fapA	A.1	ATTTGATGCGGACGAATATC	933128-933147 (CP034442)
	A.3	TAGGTTTCATTGACTGTATC	932764-932783 (CP034442)
	A.4	TGAGGTTTGTTCAAGGAGTGG	932645-932665 (CP034442)
	A.2	AGTAACTGTTAATCCAAGAGC	932253-932273 (CP034442)
	A.5	GGTGTTCCTTTCTCGG	933173-933188 (CP034442)
	A.6	AGTTAAGCTGTCCAGCTTCG	932123-932142 (CP034442)
	A.7	ACCTGCTGTAACGTATGATG	932834-932853 (CP034442)
	A.8	TAGCATTTCTAGCATCTTGC	932711-932730 (CP034442)
	A.9	AAGGAGCAAGAACCAGCAAAAC	917963-917984 (CP034442)
	A.10	TTGTGAGAATGGCGATGAGAAT	917838-917859 (CP034442)
fapB	B.1	TGCAGGATTTGTGATGACTC	1826328-1826347 (CP034442)
	B.3	GCAGGGTTGACCTTAAGGTTG	1826847-1826867 (CP034442)
	B.4	AGCAACAATATCGCAGCTGG	1826944-1826963 (CP034442)
	B.2	TCCGTACTTGCACAACATCC	1827339-1827358 (CP034442)
	B.5	TCTAGTACCCTATCAGACAC	1826236-1826255 (CP034442)
	B.6	ATTGACCACTCCTTGACCAC	1827464-1827483 (CP034442)
	B.7	ACAAGCGCAGCTCTTAGCAC	1826905-1826924 (CP034442)
	B.8	AATACACCAGCTTCAGAGTC	1827103-1827122 (CP034442)

	B.9	AGCTACATCAAGCGTCTCCATG	1841859-1841880 (CP034442)
	B.10	CGAACTTTGTGAGCCAAGATTG	1841995-1842016 (CP034442)
fapC	C.1	ACCTAGCAGCTGGTGTGATC	761428-761447 (CP034442)
	C.3	TTGTTTAGCAGTGACTTCTG	761053-761072 (CP034442)
	C.4	TATTGTGTACGCAGGAGACG	760059-760078 (CP034442)
	C.2	AACGGCTGCTAATATACGTG	759619-759638 (CP034442)
	C.5	ATCCCTTGATGTCAAGACTG	761538-761557 (CP034442)
	C.6	TAGTAATCGTATCCGTAGTC	759513-759532 (CP034442)
	C.7	TTTCAGCTGAAAGATTGGTC	761010-761029 (CP034442)
	C.8	ACCTTGAAATTGACTCAGCTG	761178-761198 (CP034442)
	C.9	GGGTGTGGAAGGCTATGTTGAG	745835-745856 (CP034442)
	C.10	CGCTGTGGTCTCTGGGAAGAT	745748-745768 (CP034442)
	C.11	GGTCGTGGGATCCCAGTGGATGCTGTTCCAGTTCCAAG[c]	760130-760152 (CP034442)
	CG.12	GCCTTATCCGTTGCTACTGCATT**CTC**TTGCCAACTATTTCTACCATTTT[d]	759782-759830 (CP034442)
	CG.13	AAAATGGTAGAAATAGTTGGCAA**GAG**AATGCAGTAGCAACGGATAAGGC[d]	759782-759830 (CP034442)
	CM.12	GCCTTATCCGTTGCTACTGCATT**CAT**TTGCCAACTATTTCTACCATTTT[d]	759782-759830 (CP034442)
	CM.13	AAAATGGTAGAAATAGTTGGCAA**ATG**AATGCAGTAGCAACGGATAAGGC[d]	759782-759830 (CP034442)
	C.14	ATGCGGCCGCTCGAGTTATTAGAAAGTTTTATAGTAATCG[c]	759502-759521 (CP034442)
	C.15	AGTAGCAACGGATAAGGCTG	759780-759799 (CP034442)
	C.16	TTGCCAACTATTTCTACCAT	759808-759827 (CP034442)
	C.17	GGTCGTGGGATCCCAGCTCAACCTGCTCCTTCAGT[c]	761648-761667 (CP034442)
	C.18	ATGCGGCCGCTCGAGTTATTAGAAAGTTTTATAGTAATCG[c]	759502-759521 (CP034442)
aad9	S.F	CGATTTTCGTTCGTGAATAC	5418–5399 (KM009065)
	S.R	TATGCAAGGGTTTATTGTTTTC	4265–4286 (KM009065)
erm	E.F	CTCGAGCGGCCGCCAGTG	264–282 (EU233623)
	E.R	AACGGCCGCCAGTGTGCTG	319–336 (EU233623)
Janus	J.F	CCGTTTGATTTTTAATGGATAATG	773–796 (AF411920.1)
	J.R	GGGCCCCTTTCCTTATGCTT	2105–2086 (AF411920.1)

rpsL	R.F	CGGTACTTTTTACTTTTGGTCTCTC	1709537-1709561 (CP034442)
	R.R	TCTTTATCCCCTTTCCTTATGC	1710075-1710096 (CP034442)

[a]Underlining indicates nucleotides introduced to allow In-fusion cloning into the pDrive vector.

[b]Underlining indicates nucleotides introduced to allow In-fusion cloning with aad9 (spectinomycin cassette).

[c]Underlining indicates nucleotides introduced to allow In-fusion cloning with pGex-5X-3 vector.

[d]Bold indicates the nucleotides altered to introduce the amino acid substitution

RESULTS

Electron microscopy images of *Streptococcus oralis* subsp. *dentisani* reveal dense mono-lateral fibrils

Electron microscopy of the *S. oralis* subsp. *dentisani* strain F0392 revealed dense mono-lateral fibrils which appeared to be of different lengths (Fig. 1). F0392 had previously been classified as *S. mitis* biovar 2 but has been reassigned to *S. oralis* subsp. *dentisani* by multilocus sequence analysis (MLSA) (9). Fibrils appeared to be composed of two different lengths, the shorter of which being approximately 300-350nm and the longer being approximately 500 nm.

This distribution of surface fibrils is similar to that seen on *Streptococcus cristatus* strains CR311 and CC5A, which also displayed mono-lateral fibrils of multiple lengths (23, 25). The long fibrils of *S. cristatus* have been linked with the SRRP SrpA.

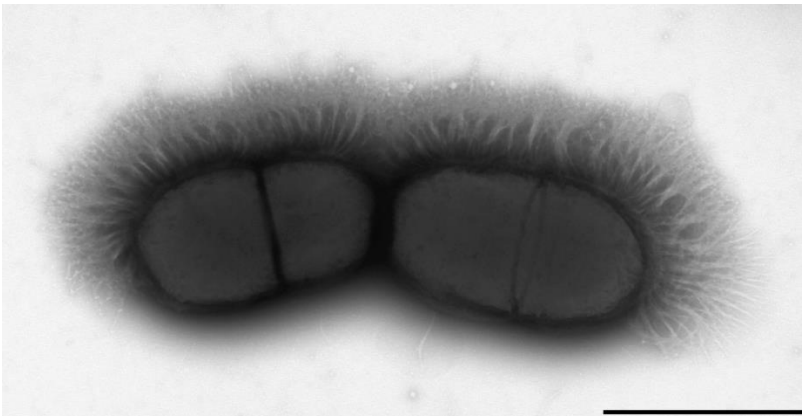

Figure 1. STEM images of *Streptococcus oralis* subsp. *dentisani* isolate F0392 bound to a formvar-coated grid and stained with 1% ammonium molybdate indicate the presence of dense mono-lateral fibrils. Scale bar, 500 nm.

Genome sequencing reveals three putative serine-rich repeat proteins

We sought to determine whether *S. oralis* subsp. *dentisani* F0392 contains genes which may encode for SRRPs. The non-contiguous F0392 genome revealed three potential genes which may encode for SRRPs; however, these sequences contained stop codons and were distributed

amongst multiple contigs, making it difficult to confirm their validity. Full genome sequencing of *S. oralis* subsp. *dentisani* strain F0392 was generated via PacBio technology, which is more capable of accurately sequencing large repeat sequences than the Illumina technology used to sequence this genome previously. Genomic analysis confirmed the presence of the three putative SRRPs open reading frames originally seen in the non-contiguous sequence. Because we predict these genes are associated with the surface fibrils on this bacterium, we have named them *fapA* (13992 bp), *fapB* (13692 bp) and *fapC* (15144 bp) for "fibril associated protein" (Fig. 2).

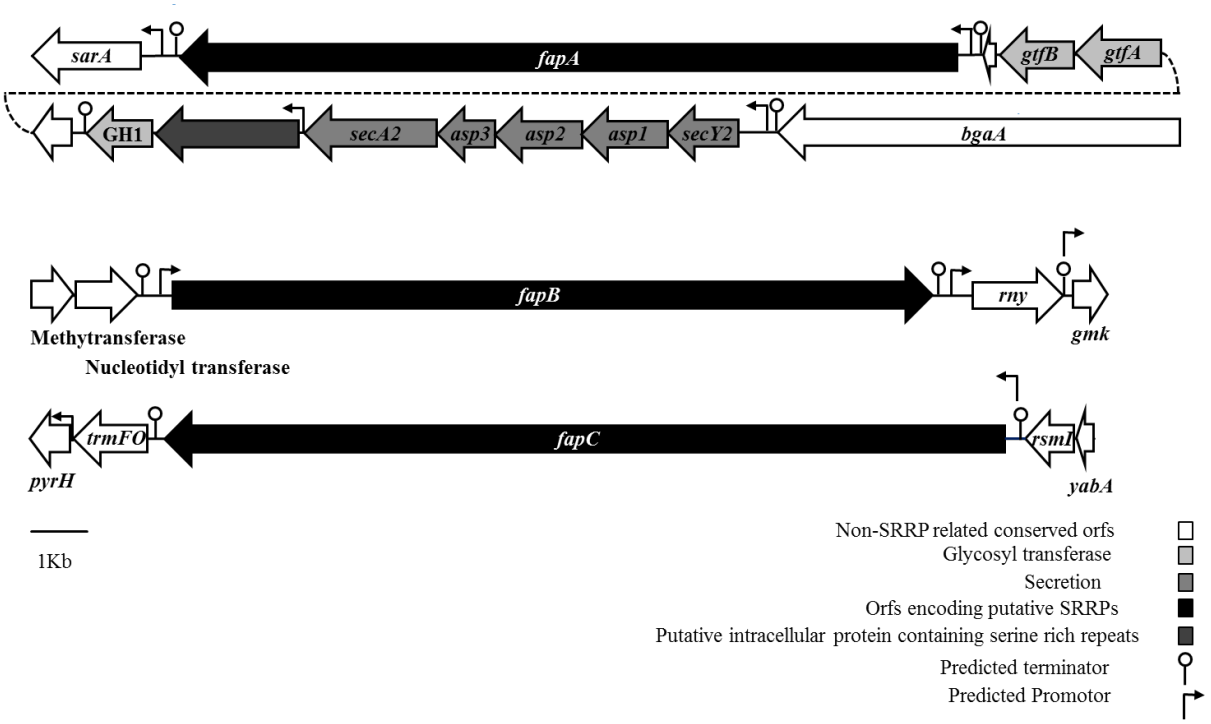

Figure 2. Schematic of loci encoding putative SRRPs in *S. oralis* subsp. *dentisani* strain F0392. Open reading frames are indicated by block arrows. Genes predicted to encode proteins of known function are labeled with gene names, if known, or predicted function.
Indicates predicted terminators and indicates predicted promoters.

Each of these three open-reading frames is predicted to encode a protein containing the conserved features of previously identified SRRPs, including an atypical N-terminal signal sequence, a cell wall anchor domain and two serine-repeat regions which flank a non-repeat region (13, 17, 23, 32, 40-45). The atypical N-terminal signal sequence is responsible for secretion of the protein via the accessory secretion system (SecA2/Y2) and is generally

approximately 90 amino acids long (41). The putative SRRPs encoded for within *S. oralis* subsp. *dentisani* F0392 contain predicated signal sequences of 93 amino acids in length, which are highly conserved between the three SRRPs, showing 100% amino acid identity between FapA and FapB and 93.5% identity with FapC. The N-terminal sequence similarity between FapA and FapB extends past this region, having 80% identity and 82% similarity between the first 338 amino acids of FapA and the first 348 amino acids of FapB. FapC does not share this similarity with either FapA or FapB apart from the atypical signal sequence.

It is also important to note that *fapA* is located at the 3' end of an operon which also contains genes encoding for proteins responsible for glycosylation and secretion of the SRRP. The regions containing *fapB* and *fapC* do not contain any other genes related to SRRPs (Fig. 2).

Predicted SRRP contribution to observed surface fibrils

In order to determine whether the surface fibrils of F0392 were dependent upon one or more of the predicted SRRP encoding genes, we took advantage of the accessory secretion system specific for secretion of SRRPs. An insertion-deletion mutant was generated which lacked *secA2*, the gene which encodes for the ATPase which energizes SRRP transport across the membrane (27, 40). This mutant lacks all fibrils, supporting the hypothesis that these fibrils are SRRPs and SecA2 dependent (Fig. 3). Single, double and triple mutants were then generated in order to determine the contribution of each open-reading frame to the presence of surface fibrils. Imaging of double mutants revealed that each of the mutants retained presence of surface fibrils, suggesting that all three of the putative SRRPs are produced. Interestingly, each of the three SRRPs yielded a different density and distribution of surface fibrils across the occupied side (Fig. 3). The mutant expressing only FapB (F0392 Δ*fapC*Δ*fapA*) displayed fibrils which were similar in appearance to the parental strain. The FapA expressing mutant (F0392 Δ*fapC*Δ*fapB)*

also displayed fibrils resembling the parent, however, these fibrils appeared less dense than those of the parental strain. The fibrils on the FapC expressing mutant (F0392 Δ*fapB*Δ*fapA*) were mostly concentrated toward the poles of the cells and localized on the oldest cells in the chain (data not shown). A triple mutant, F0392 Δ*fapC*Δ*fapB*Δ*fapA*, was devoid of surface fibrils, confirming that these SRRP encoding genes were necessary to produce surface fibrils (Fig. 3).

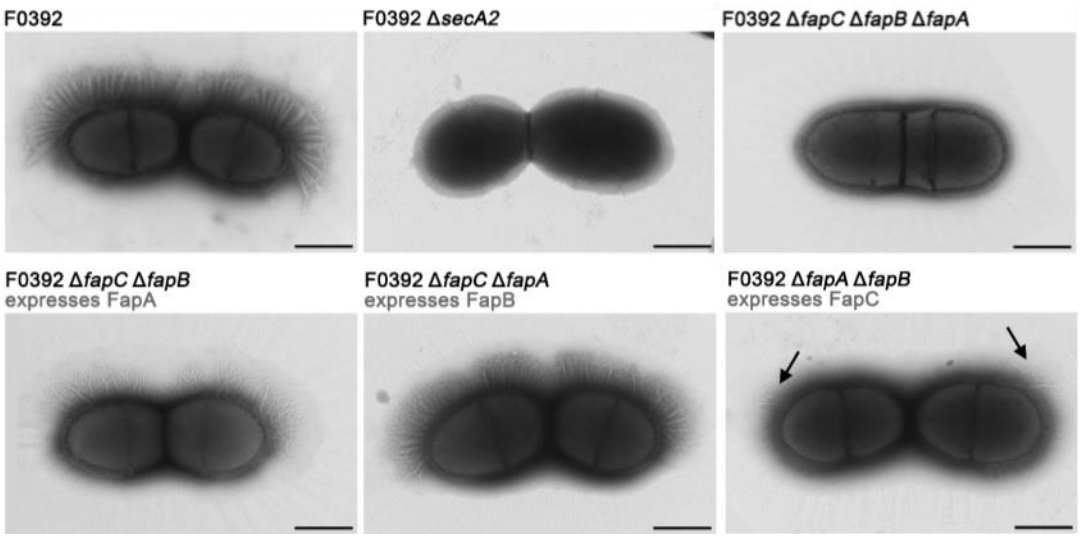

Figure 3. Three SRRPs contribute to production of fibrils on the surface of *S. oralis* subsp. *dentisani* strain F0392. STEM images of the parental strain, F0392, and the generated mutants bound to a formvar-coated grid and stained with 1% ammonium molybdate. Strain names are above the panels in black and the SRRPs still expressed in each double mutant are given in grey (scale bar, 500 nm).

Predicted SRRP functions

In order to determine possible functions of FapA, B and C, the amino acid sequences of the NRR of each SRRP were compared against NRR sequences of known SRRPs with identified catalytic domains and functions (Fig. 4).

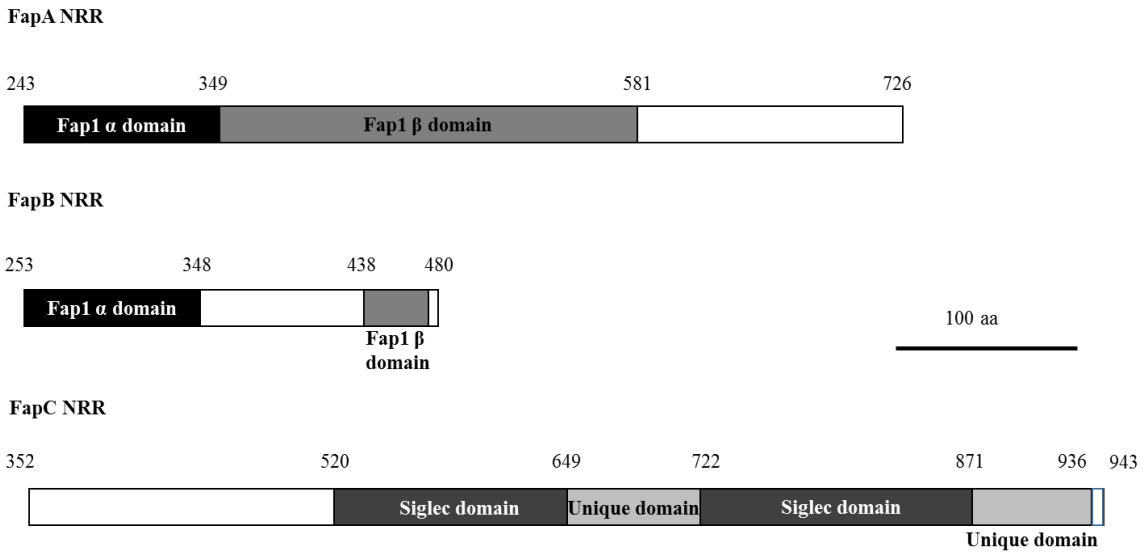

Figure 4. Schematic illustration of the putative domains within the NRR of *S. oralis* subsp. *dentisani* F0392 SRRPs. Domains identified by HHpred, a server for remote homolog detection, are labeled. The numbers above the schematics indicate the predicted boundaries of the domains. There were small differences in the boundaries predicted for the domains within FapC using structures of *S. gordonii* GspB and *S. sanguinis* SrpA. The boundaries provided here are from the prediction using SrpA. In addition, the boundaries identified resulted in an overlap of seven amino acids (722-729) between the first unique domain and second Siglec domain.

The NRR of FapA shared 90% amino acid identity and 93% similarity with the SRRP SrpA from *S. cristatus* CC5A. *srpA* dependent fibrils have been implicated in being necessary for the formation of 'corncob' structures with species such as *Corynebacterium matruchotti* and *Fusobacterium nucleatum*, although the specific receptor involved in this interaction is unknown (23-25). Corncob structures are prominent in dental biofilms and are thought to anchor the non-streptococcal structures to the tooth surface (46-48). Sequence similarity between SrpA and FapA suggests FapA may play a role in interspecies interactions such as corncob formation. Additionally, we have identified an open reading frame in *S. cristatus* CR311 which encodes for a protein that shares 93% identity and 95% amino acid similarity with the FapC NRR.

HHpred, a server which detects homologs using structural information, identified structural similarity between FapA and *S. parasanguinis* SRRP Fap1 (97.8% probability, E-value $8.5x10^{-8}$) (PDB ID: 2X12) (31, 49). Fap1 contains two catalytic domains which have both been shown to

contribute to adhesion, α (aa 129-206) and β (aa 237-425) (31). These domains are conserved in the NRR of FapA (Fig. 4). Because FapA and FapB share N-terminal sequence similarity, there is also some sequence similarity between their NRRs and therefore some predicted structural similarity between the two regions. Thus, FapB also shares predicted structural similarity with *S. parasanguinis* Fap1, covering the Fap1 α domain (92% probability, E-value $4.5x10^{-3}$) (PDB ID: 2KUB) (31) (Fig. 4). The 3' region of the FapB NRR also shares some predicted structural similarity with the C-terminal region of the Fap1 β domain (65.2% probability, E-value 4.6) (PDB ID: 2X12). *S. parasanguinis* Fap1 has been shown to be required for efficient binding to saliva coated hydroxyapatite and biofilm formation, suggesting a role for FapA and FapB in these functions (32, 33, 50).

FapC was predicted to share structural similarity with sialic acid binding immunoglobulin-like lectins (Siglecs) and unique domains from *S. sanguinis* and *S. gordonii* (PDB IDs: 3QC5 and 5KIQ) (>99% probability, E-value > $1x10^{-14}$) (49, 51, 52). Interestingly, FapC contains two of each of these domains (Fig. 4). *S. sanguinis* SK1 has been reported to also contain two of each of these domains, however only one of the two Siglecs was predicted to contain the active arginine residue necessary to bind sialic acid in other bacterial Siglecs (51, 53, 54). This is also the case in FapC. It is unknown whether the other Siglec domain in SK1 or FapC, which lacks the predicted active arginine residue, contributes to adhesion. However, the NRR of SK1 has been shown to bind sialic acid, implicating a role for FapC in sialic acid binding (53).

FapC is necessary for effective adherence to saliva

As sialic acid is a widely distributed host receptor and would be important in both oral colonization and infective endocarditis, we sought to determine the ability of this bacterium to bind sialic acid, specifically the contribution of FapC, which is predicted to contain Siglec

domains. Study of adherence to immobilized saliva was chosen as saliva is heavily sialylated and it is unlikely that bacterial adhesion to free sialic acid plays a role in colonization or infection (55). F0392 Δ*fapC* showed a significant reduction (>90%) in adherence relative to the parental strain, suggesting FapC does bind sialic acid (Fig. 5A). A second independent FapC mutant was also reduced in binding (8.1% ± 3.4% of parental adhesion).

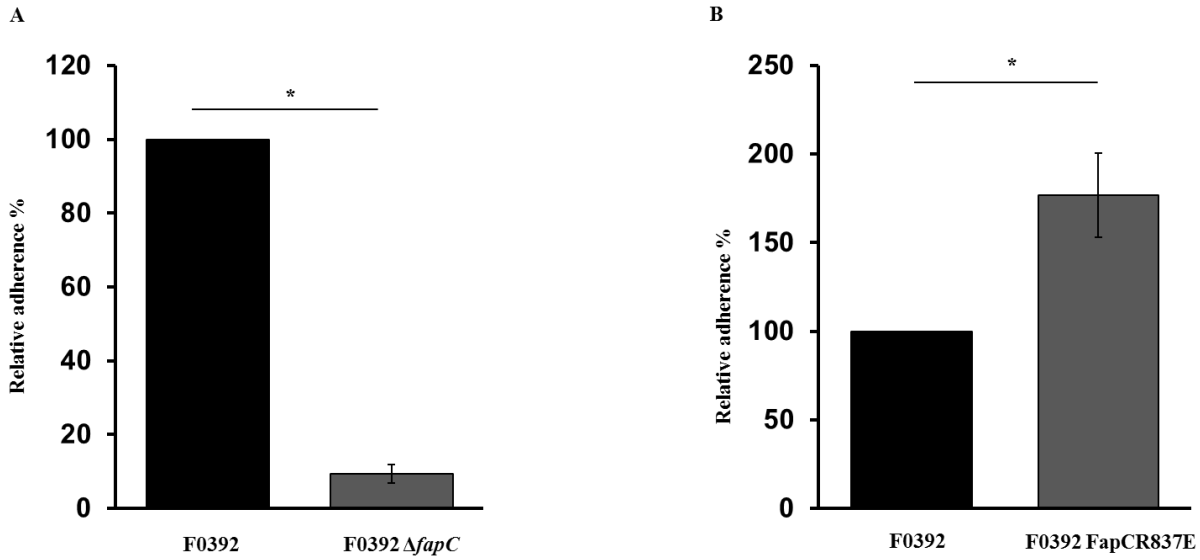

Figure 5. The contribution *S. oralis* subsp. *dentisani* strain F0392 SRRP FapC to saliva binding. FapC is required for efficient binding to saliva (A). However, mutation of a conserved arginine residue shown in other Siglec domains to be required for sialic acid binding increases adhesion (B). Adhesion is expressed as a percentage relative to that of the parental strain. Values are the mean of at least three independent experiments each performed in triplicate ±SD. Statistical significance was tested by a two-tailed Student's t test; *, $P \leq 0.01$.

To further study this interaction, a point mutant, F0392 FapCR837E, was generated in which the predicted active arginine residue was changed to glutamic acid. As this change has previously been shown to eliminate sialic acid binding in other SRRPs, we expected this point mutant to bind saliva less efficiently than the parent (52-54). Interestingly, an increase in saliva binding was observed for the F0392 FapCR837E mutant compared to the wild type (Fig. 5B). As FapA contains two predicted Siglec domains within its NRR, it possible that there is a residue within the other Siglec domain that is able to bind to sialic acid.

To determine whether the interaction between F0392 FapC and saliva was direct, the NRR of FapC was recombinantly expressed and used to test if addition of this region would competitively inhibit binding of F0392. Results show that addition of recombinant $FapC_{217-938}$ does reduce adherence of F0392 to levels similar to that of F0392 Δ*fapC* (Fig. 6). Furthermore, adherence of F0392 Δ*fapC* was not further reduced by the addition of recombinant $FapC_{217-938}$. These data suggest that the FapC-saliva interaction is direct.

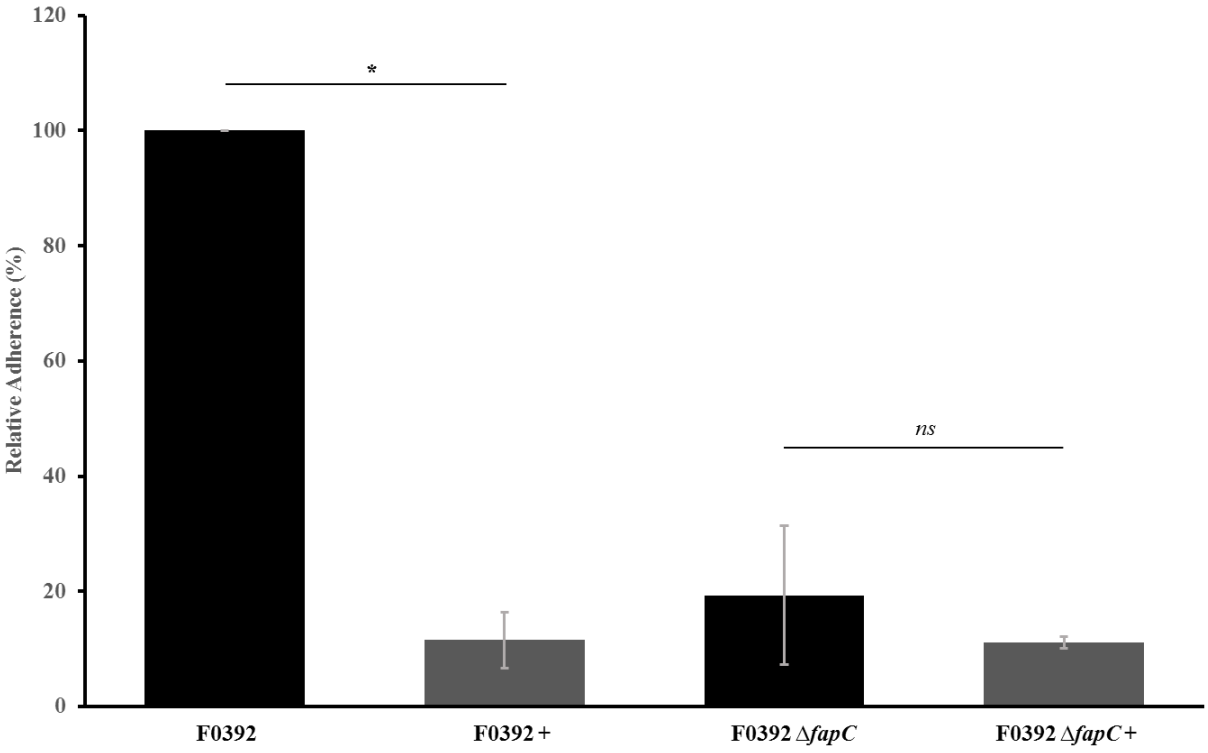

Figure 6. Adhesion of F0392 FapC to saliva is a direct interaction. "+" indicates trials in which 5-7 µM $rFapC_{217-938}$ was added. Adhesion is expressed as a percentage relative to that of the parental strain. Values are the mean of at least three independent experiments each performed in triplicate ±SD. Statistical significance was tested by a two-tailed Student's t test; *, $P \leq 0.01$; *ns*, not significant.

In order to better understand whether FapC was binding sialic acid, saliva adherence assays were conducted in which saliva was pre-treated with *Clostridium perfrigens* neuraminidase in order to

cleave terminal sialic acid receptors present on saliva. Somewhat unexpectedly, binding of F0392 to neuraminidase treated saliva was not significantly different from binding to untreated saliva (Fig. 7). These data seem to suggest that the SRRPs produced by this strain are able to bind carbohydrate receptors underlying sialic acid.

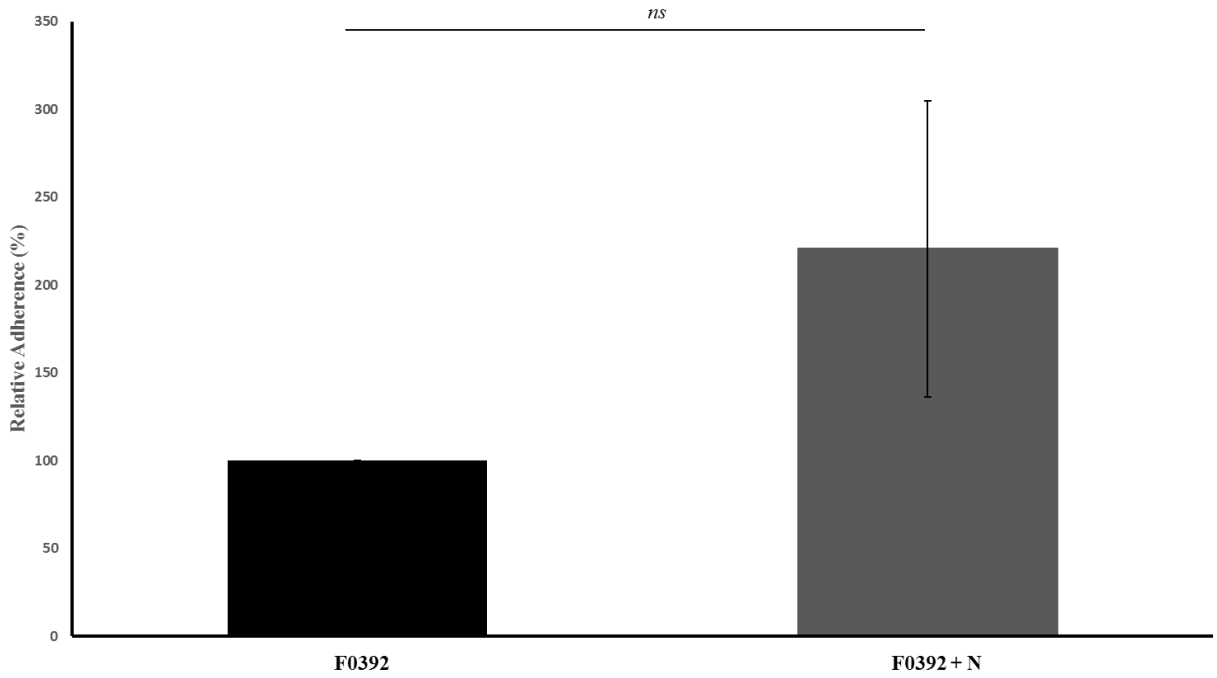

Figure 7. Cleavage of terminal sialic acid does not decrease adhesion of F0392 to bound saliva as predicted. This suggests that SRRPs of F0392 may be able to bind carbohydrates underlying sialic acid. Adhesion is expressed as a percentage relative to that of the parental strain. Values are the mean of at least three independent experiments each performed in triplicate ±SD. Statistical significance was tested by a two-tailed Student's t test; *ns*, not significant.

To further study whether FapC was binding sialic acid, blocking assays were conducted in which free sialic acid was added to saliva binding assays to test its ability to block interactions between saliva and FapC. Results show that there is no significant difference in saliva binding when sialic acid is added (Fig. 8). This may indicate that F0392 not able to bind free sialic acid.

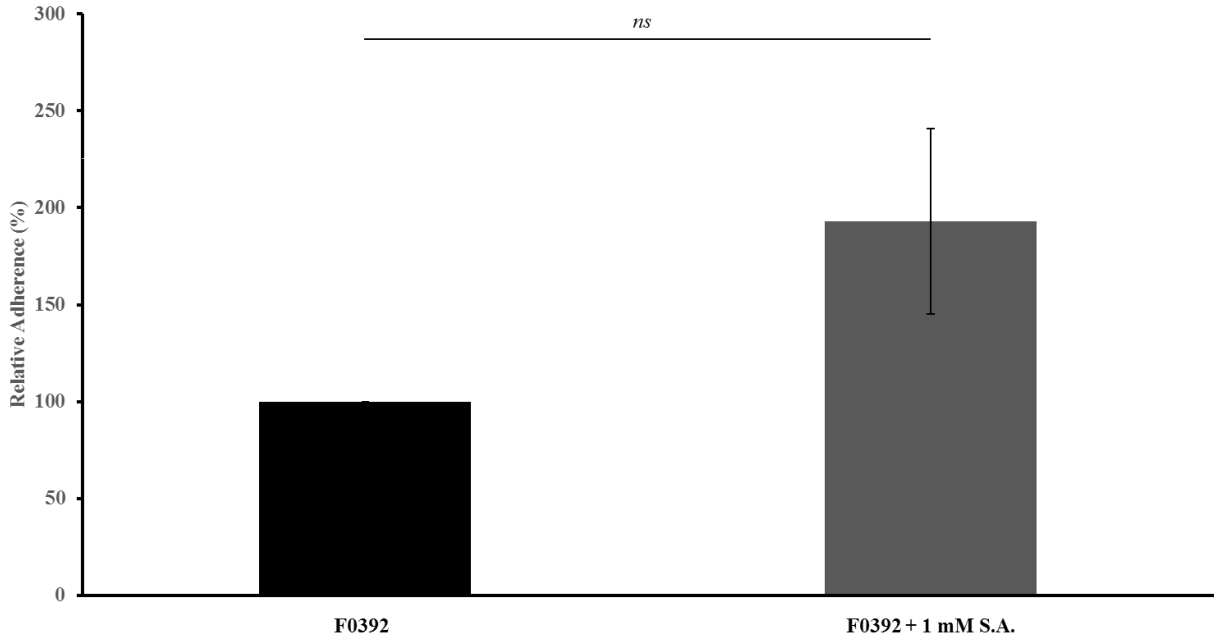

Figure 8. Addition of free sialic acid does not significantly impact adhesion of F0392 to saliva. Adhesion is expressed as a percentage relative to that of the parental strain. Values are the mean of at least three independent experiments each performed in triplicate ±SD. Statistical significance was tested by a two-tailed Student's t test; *ns*, not significant.

As FapA and FapB are predicted to play a part in intraspecies interactions, auto-aggregation assays were conducted in order to test their role in F0392 aggregation. Results showed that FapA, FapB and FapC may to contribute to the ability of F0392 to aggregate. F0392 Δ*fapA*, F0392 Δ*fapC*Δ*fapB*, F0392 Δ*fapB*Δ*fapA* and F0392 Δ*fapC*Δ*fapB*Δ*fapA* all show significantly less aggregation than the parental strain. Aggregation of F0392 Δ*fapB* was not significantly different from the parental strain, however given that aggregation of the *fapB* mutant was reduced in each of three experiments, we predict further testing will show this difference is significant. Each of the three double mutants showed significantly higher aggregation than the triple mutant, indicating that the presence of any one SRRP may be enough to cause aggregation to some degree. Significant differences between the double mutants expressing FapA or FapB and the double mutant expressing FapC show that the relative contributions of each of the

SRRPs to aggregation may be different.

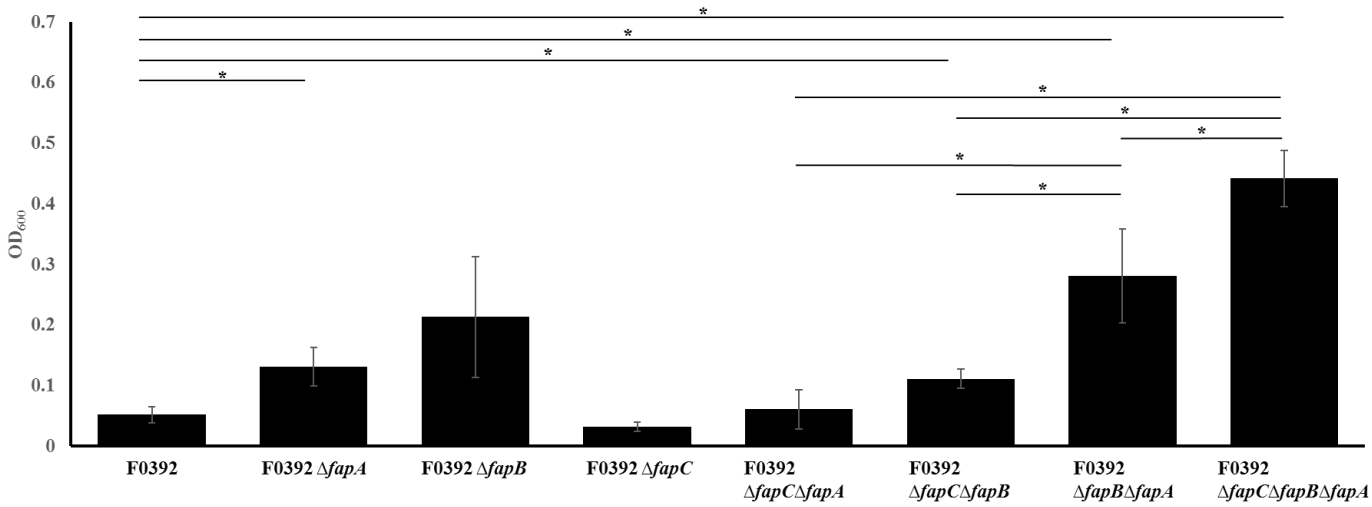

Figure 9. FapA and FapB contribute to auto-aggregation of F0392. Aggregation is measured by absorbance at 600 nm post 2-hour incubation while shaking. Values are the mean of at least three independent experiments ±SD. Statistical significance was tested by a two-tailed Student's t test; *, $P \leq 0.05$.

DISCUSSION

In this study, we have identified a *Streptococcus oralis* subsp. *dentisani* oral isolate (F0392) which produces three serine-rich repeat proteins, resulting in the formation of dense mono-lateral fibrils on the cell surface. We have demonstrated that one of these proteins, FapC, is necessary for efficient binding to saliva and a combination of these proteins appear to play a role in auto-aggregation.

Although it is unusual for streptococcal strains to express more than a single SRRP, there have been other cases of the expression of multiple SRRPs similar to *S. oralis* subsp. *dentisani*. *Streptococcus salivarius* has been shown to also express three SRRPs, although these SRRPs are distributed evenly across the bacterial surface (13). Mono-lateral fibrils of multiple lengths have also been observed on *S. cristatus* strains CR311 and CC5A. The longer one of these fibrils has been correlated to the SRRP SrpA (23, 25). We have also identified an additional SRRP encoding gene within the CR311 genome (AFUE01000008). The 90% amino acid identity and

93% similarity between the NRRs of FapA and the *S. cristatus* SRRP SrpA as well as the 93% amino acid identity and 95% similarity between the NRR of FapC and a putative protein of *S. cristatus* CR311 suggests there may have been multiple recombination events between these two species (9). *S. cristatus* is not as closely related to *S. oralis* subsp. *dentisani* as some other organisms, making it likely that these species have undergone horizontal gene transfer, as they are the only two identified streptococci with mono-lateral fibrils.

The same study which identified mono-lateral fibrils of *S. cristatus* also described mono-lateral fibrils for *S. oralis*; however, because of changes in classification of this species, it is unclear whether this is the same *S. oralis* described today (23). Additionally, some *Geobacter* species, including *G. metallireducens*, produce mono-lateral pili on the surface of their cells (56). The mechanism of fibril/pili localization for these species is unknown. The FapA encoding locus also contains genes encoding for proteins responsible for glycosylation and secretion of SRRPs. We hypothesize that genes in this locus may be controlling the distribution of the accessory secretion system, SecA2/Y2, thus producing this mono-lateral distribution.

Imaging of F0392 double mutants, which only express a single SRRP, showed observable differences in the distribution of each fibril on the bacterial surface (Fig. 3). The mechanism for this difference in distribution is unknown, although we hypothesize it may be due to differences in timing and/or levels of *fap* gene expression, as well as the conditions required for secretion via the accessory Sec system. Although the mechanism is not yet known, we believe the presence of differentially distributed surface fibrils on all three double mutants indicates that each SRRP produces a distinct fibril, although we cannot rule out the possibility that fibrils observed on the parental strain consist of more than one fibrillar protein. Images of the parental strain showed fibrils which appeared to be of two different lengths, leading us to believe that at least one of the

SRRPs produce a longer fibril; however, the double mutants did not appear to show any differences in length between fibrils (Fig. 3). It is possible that the decrease in fibril density of the double mutants caused less stain to be trapped, making it more difficult to visualize fibrils which are further from the bacterial surface. Alternatively, fewer fibrils may relax the physical constrains the fibrils place on each other, thus allowing them to extend further from the bacterial surface.

All identified functions of SRRPs have centered on bacterial adhesion through the proteins non-repeat region. We hypothesize that these proteins play a major role in the ability of *S. oralis* subsp. *dentisani* to colonize the oral cavity, as this species is adapted to colonize this environment. Study of sequence similarity between the NRR of FapA and the NRR of other known SRRPs suggests that FapA mediates interspecies interactions. Structural predictions of the NRR reveal that FapA and FapB may contribute to biofilm formation, while FapC may contribute to sialic acid binding. Structural prediction identified two putative Siglec and unique domains in the FapC NRR. These domains have been known to be required for sialic acid binding in other SRRPs (17, 52, 53, 57, 58). We chose to further study the role of FapC to sialic acid binding as sialic acid is a widely distributed host receptor and would likely play a role in oral colonization, as many tooth and other oral surfaces are coated in salivary glycoproteins which are often heavily sialylated. Only one of the two putative Siglec domains in the FapC NRR contains the predicted active arginine residue reported to be critical in sialic acid binding (51, 53, 54). Previous studies have shown that mutation of this residue to glutamic acid eliminates sialic acid binding (51, 53, 54). However, mutation of this residue in FapC actually caused an increase in adherence (Fig. 5). It is proposed that this arginine residue facilitates adhesion by hydrogen bonding with the glycerol group of sialic acid (59). As glutamic acid is

capable of hydrogen bonding, it is possible that the binding pocket can accommodate this change and still position the ligand correctly to allow hydrogen bonding. Substantiating this, hydrogen bonding between sialic acid glycerol and an acidic residue has been observed, including viral and bacterial neuraminidases (60, 61). Another member of the lab generated and tested adherence of an arginine to methionine point mutant to assess this theory, however, there was no significant change in adherence, leaving much of the mechanism of this interaction unclear.

Although FapA and FapB are predicted to share structural similarity with *S. parasanguinis* SRRP Fap1, which was required for efficient binding to saliva coated hydroxyapatite and biofilm formation (32, 33, 50). The large decrease in adherence of the FapC mutant indicates that if FapA or FapB contribute to saliva binding, this contribution must be relatively small. However, FapA or FapB may bind carbohydrates underlying sialic acid. The non-significant difference in adherence to neuraminidase treated saliva suggests that F0392 is able to bind carbohydrates underlying sialic acid (Fig. 7). It is unclear as to whether one or multiple SRRPs produced by F0392 are able to bind underlying carbohydrates, but strains producing sialic acid binding SRRPs have been shown to also bind cryptic β-1,4 linked galactose exposed by endogenous neuraminidase (17, 18).

Sialic acid blocking has previously been shown to decrease adherence of sialic acid binding SRRPs to platelets (17). It was thus surprising that adherence of F0392 was not significantly reduced by addition of free sialic acid (Fig. 8). However, this does not eliminate the possibility that FapC is binding sialic acid. It is possible that FapC is unable to bind free sialic acid, but rather requires sialic acid to be a terminal receptor on a chain of carbohydrates or only binds particular linkages of sialic acid.

Upon testing of interspecies interactions of F0392 wild-type and mutant strains, we noticed differences in aggregation of the F0392 wild-type and triple mutant control groups. This led to the hypothesis that the fibrils may be impacting the ability of this bacterium to auto-aggregate. As predicted domains in FapA and FapB are thought to be involved in intraspecies interactions, we designed an auto-aggregation assay to test the ability of each mutant to aggregate. FapA and FapB seem to be the primary contributors to this interaction. The significant reduction in aggregation from the parental strain to the FapA mutant implicates this protein in aggregation. Although the change in aggregation between the parental strain and the FapB mutant was not significant, we expect that further testing will show that removal of FapB does result in a significant decrease in aggregation. The involvement of FapA and FapB is further supported by the significantly higher aggregation of the double mutants which only express FapA or FapB compared to the FapC expressing double mutant. This would suggest that if FapC only plays a role in aggregation when it is the only SRRP present. Furthermore, significant differences between each of the double mutants and the triple mutant suggests that removal of either FapA, FapB or FapC impacts aggregation, with removal of FapC appearing to have the smallest effect. Finally, the non-significant difference between the parental strain and FapB expressing mutant suggests FapB alone may be enough to cause aggregation. The exact contribution of FapA, FapB and FapC to F0392 auto-aggregation is unclear, but these data suggest that FapA and FapB both likely play a role.

Through this work we have established that *S. oralis* subsp. *dentisani* produces dense mono-lateral fibrils. Our data supports our hypothesis that this organism produces three distinct fibrils of different distributions across the cell surface, each of which is linked to a SRRP. Although the exact function of each of these SRRPs is unknown, predicted domains suggest they each play a

unique role in bacterial adhesion. We have shown that at least one of these SRRPs is necessary for efficient binding to saliva, and others appear to influence auto-aggregation. As the mono-lateral distribution of fibrils and expression of multiple SRRPs is a relatively unstudied phenomenon, more work will need to be done in order to better understand the functions of these proteins and the effect of their distribution on cell biology before we can begin to understand their clinical significance or potential role in infective endocarditis.

REFERENCES

1. McDonald JR. 2009. Acute infective endocarditis. Infect Dis Clin North Am 23:643-64.
2. Bashore TM, Cabell C, Fowler V, Jr. 2006. Update on infective endocarditis. Curr Probl Cardiol 31:274-352.
3. Werdan K, Dietz S, Loffler B, Niemann S, Bushnaq H, Silber RE, Peters G, Muller-Werdan U. 2014. Mechanisms of infective endocarditis: pathogen-host interaction and risk states. Nat Rev Cardiol 11:35-50.
4. Mylonakis E, Calderwood SB. 2001. Infective Endocarditis in Adults. New England Journal of Medicine 345:1318-1330.
5. Bor DH, Woolhandler S, Nardin R, Brusch J, Himmelstein DU. 2013. Infective endocarditis in the U.S., 1998-2009: a nationwide study. PLoS One 8:e60033.
6. Kumar VN, van der Linden M, Menon T, Nitsche-Schmitz DP. 2014. Viridans and bovis group streptococci that cause infective endocarditis in two regions with contrasting epidemiology. International Journal of Medical Microbiology 304:262-268.
7. Westling K, Julander I, Ljungman P, Vondracek M, Wretlind B, Jalal S. 2008. Identification of species of viridans group streptococci in clinical blood culture isolates by sequence analysis of the RNase P RNA gene, *rnpB*. Journal of Infection 56:204-210.
8. Bishop CJ, Aanensen DM, Jordan GE, Kilian M, Hanage WP, Spratt BG. 2009. Assigning strains to bacterial species via the internet. BMC Biol 7:3.
9. Jensen A, Scholz CF, Kilian M. 2016. Re-evaluation of the taxonomy of the Mitis group of the genus *Streptococcus* based on whole genome phylogenetic analyses, and proposed reclassification of *Streptococcus dentisani* as *Streptococcus oralis* subsp. *dentisani* comb. nov., *Streptococcus tigurinus* as *Streptococcus oralis* subsp. *tigurinus* comb. nov., and *Streptococcus oligofermentans* as a later synonym of *Streptococcus cristatus*. Int J Syst Evol Microbiol 66:4803-4820.
10. Rasmussen LH, Hojholt K, Dargis R, Christensen JJ, Skovgaard O, Justesen US, Rosenvinge FS, Moser C, Lukjancenko O, Rasmussen S, Nielsen XC. 2017. In silico assessment of virulence factors in strains of *Streptococcus oralis* and *Streptococcus mitis* isolated from patients with Infective Endocarditis. J Med Microbiol doi:10.1099/jmm.0.000573.
11. Washburn MR, White JC, Niven CF, Jr. 1946. Streptococcus S.B.E.: Immunological Characteristics. J Bacteriol 51:723-9.
12. Zbinden A, Mueller NJ, Tarr PE, Sproer C, Keller PM, Bloemberg GV. 2012. *Streptococcus tigurinus* sp. nov., isolated from blood of patients with endocarditis, meningitis and spondylodiscitis. Int J Syst Evol Microbiol 62:2941-5.
13. Couvigny B, Lapaque N, Rigottier-Gois L, Guillot A, Chat S, Meylheuc T, Kulakauskas S, Rohde M, Mistou MY, Renault P, Dore J, Briandet R, Serror P, Guedon E. 2017. Three glycosylated serine-rich repeat proteins play a pivotal role in adhesion and colonization of the pioneer commensal bacterium, *Streptococcus salivarius*. Environ Microbiol 19:3579-3594.
14. Lizcano A, Sanchez CJ, Orihuela CJ. 2012. A role for glycosylated serine-rich repeat proteins in gram-positive bacterial pathogenesis. Mol Oral Microbiol 27:257-69.
15. Seo HS, Mu R, Kim BJ, Doran KS, Sullam PM. 2012. Binding of glycoprotein Srr1 of *Streptococcus agalactiae* to fibrinogen promotes attachment to brain endothelium and the development of meningitis. PLoS Pathog 8:e1002947.
16. Sequeira S, Kavanaugh D, MacKenzie DA, Suligoj T, Walpole S, Leclaire C, Gunning AP, Latousakis D, Willats WGT, Angulo J, Dong C, Juge N. 2018. Structural basis for the role of serine-rich repeat

proteins from *Lactobacillus reuteri* in gut microbe-host interactions. Proc Natl Acad Sci U S A 115:E2706-E2715.
17. Singh AK, Woodiga SA, Grau MA, King SJ. 2017. *Streptococcus oralis* Neuraminidase Modulates Adherence to Multiple Carbohydrates on Platelets. Infect Immun 85.
18. Wong A, Grau MA, Singh AK, Woodiga SA, King SJ. 2018. Role of Neuraminidase-Producing Bacteria in Exposing Cryptic Carbohydrate Receptors for *Streptococcus gordonii* Adherence. Infect Immun 86.
19. Samen U, Eikmanns BJ, Reinscheid DJ, Borges F. 2007. The surface protein Srr-1 of *Streptococcus agalactiae* binds human keratin 4 and promotes adherence to epithelial HEp-2 cells. Infect Immun 75:5405-14.
20. Schulte T, Mikaelsson C, Beaussart A, Kikhney A, Deshmukh M, Wolniak S, Pathak A, Ebel C, Lofling J, Fogolari F, Henriques-Normark B, Dufrene YF, Svergun D, Nygren PA, Achour A. 2016. The BR domain of PsrP interacts with extracellular DNA to promote bacterial aggregation; structural insights into pneumococcal biofilm formation. Sci Rep 6:32371.
21. Shivshankar P, Sanchez C, Rose LF, Orihuela CJ. 2009. The *Streptococcus pneumoniae* adhesin PsrP binds to Keratin 10 on lung cells. Mol Microbiol 73:663-79.
22. Schulte T, Lofling J, Mikaelsson C, Kikhney A, Hentrich K, Diamante A, Ebel C, Normark S, Svergun D, Henriques-Normark B, Achour A. 2014. The basic keratin 10-binding domain of the virulence-associated pneumococcal serine-rich protein PsrP adopts a novel MSCRAMM fold. Open Biol 4:130090.
23. Handley PS, Correia FF, Russell K, Rosan B, DiRienzo JM. 2005. Association of a novel high molecular weight, serine-rich protein (SrpA) with fibril-mediated adhesion of the oral biofilm bacterium *Streptococcus cristatus*. Oral Microbiol Immunol 20:131-40.
24. Lancy P, Jr., Dirienzo JM, Appelbaum B, Rosan B, Holt SC. 1983. Corncob formation between *Fusobacterium nucleatum* and *Streptococcus sanguis*. Infect Immun 40:303-9.
25. Mouton C, Reynolds HS, Genco RJ. 1980. Characterization of tufted streptococci isolated from the "corn cob" configuration of human dental plaque. Infect Immun 27:235-45.
26. Sanchez CJ, Shivshankar P, Stol K, Trakhtenbroit S, Sullam PM, Sauer K, Hermans PW, Orihuela CJ. 2010. The pneumococcal serine-rich repeat protein is an intra-species bacterial adhesin that promotes bacterial aggregation in vivo and in biofilms. PLoS Pathog 6:e1001044.
27. Bensing BA, Seepersaud R, Yen YT, Sullam PM. 2014. Selective transport by SecA2: an expanding family of customized motor proteins. Biochim Biophys Acta 1843:1674-86.
28. Zhou M, Wu H. 2009. Glycosylation and biogenesis of a family of serine-rich bacterial adhesins. Microbiology 155:317-27.
29. Chen Y, Seepersaud R, Bensing BA, Sullam PM, Rapoport TA. 2016. Mechanism of a cytosolic *O*-glycosyltransferase essential for the synthesis of a bacterial adhesion protein. Proc Natl Acad Sci U S A 113:E1190-9.
30. Latousakis D, Juge N. 2018. How Sweet Are Our Gut Beneficial Bacteria? A Focus on Protein Glycosylation in *Lactobacillus*. Int J Mol Sci 19.
31. Ramboarina S, Garnett JA, Zhou M, Li Y, Peng Z, Taylor JD, Lee WC, Bodey A, Murray JW, Alguel Y, Bergeron J, Bardiaux B, Sawyer E, Isaacson R, Tagliaferri C, Cota E, Nilges M, Simpson P, Ruiz T, Wu H, Matthews S. 2010. Structural insights into serine-rich fimbriae from Gram-positive bacteria. J Biol Chem 285:32446-57.
32. Wu H, Fives-Taylor PM. 1999. Identification of dipeptide repeats and a cell wall sorting signal in the fimbriae-associated adhesin, Fap1, of *Streptococcus parasanguis*. Mol Microbiol 34:1070-81.
33. Wu H, Mintz KP, Ladha M, Fives-Taylor PM. 1998. Isolation and characterization of Fap1, a fimbriae-associated adhesin of *Streptococcus parasanguis* FW213. Mol Microbiol 28:487-500.

34. Handley PS, Carter PL, Wyatt JE, Hesketh LM. 1985. Surface structures (peritrichous fibrils and tufts of fibrils) found on *Streptococcus sanguis* strains may be related to their ability to coaggregate with other oral genera. Infect Immun 47:217-27.
35. Correia FF, DiRienzo JM, Lamont RJ, Anderman C, McKay TL, Rosan B. 1995. Insertional inactivation of binding determinants of *Streptococcus crista* CC5A using Tn916. Oral Microbiol Immunol 10:220-6.
36. Joeseph MD, Frederick FC, Richard L, Manfred EB, Burton R. 1997. Cloning and Sequencing of a Mutated Locus That Affects Fimbrial Tuft Organization and Corncob Formation in *Streptococcus crista* CC5A. International Journal of Oral Biology 22:241-248.
37. Lacks S, Hotchkiss RD. 1960. A study of the genetic material determining an enzyme in *Pneumococcus*. Biochim Biophys Acta 39:508-18.
38. Sung CK, Li H, Claverys JP, Morrison DA. 2001. An *rpsL* cassette, janus, for gene replacement through negative selection in *Streptococcus pneumoniae*. Appl Environ Microbiol 67:5190-6.
39. Allan RN, Skipp P, Jefferies J, Clarke SC, Faust SN, Hall-Stoodley L, Webb J. 2014. Pronounced metabolic changes in adaptation to biofilm growth by *Streptococcus pneumoniae*. PLoS One 9:e107015.
40. Bensing BA, Sullam PM. 2002. An accessory sec locus of *Streptococcus gordonii* is required for export of the surface protein GspB and for normal levels of binding to human platelets. Mol Microbiol 44:1081-94.
41. Bensing BA, Takamatsu D, Sullam PM. 2005. Determinants of the streptococcal surface glycoprotein GspB that facilitate export by the accessory Sec system. Mol Microbiol 58:1468-81.
42. Rose L, Shivshankar P, Hinojosa E, Rodriguez A, Sanchez CJ, Orihuela CJ. 2008. Antibodies against PsrP, a novel *Streptococcus pneumoniae* adhesin, block adhesion and protect mice against pneumococcal challenge. J Infect Dis 198:375-83.
43. Schneewind O, Mihaylova-Petkov D, Model P. 1993. Cell wall sorting signals in surface proteins of gram-positive bacteria. EMBO J 12:4803-11.
44. Siboo IR, Chambers HF, Sullam PM. 2005. Role of SraP, a Serine-Rich Surface Protein of *Staphylococcus aureus*, in binding to human platelets. Infect Immun 73:2273-80.
45. Takahashi Y, Konishi K, Cisar JO, Yoshikawa M. 2002. Identification and characterization of *hsa*, the gene encoding the sialic acid-binding adhesin of *Streptococcus gordonii* DL1. Infect Immun 70:1209-18.
46. Jones SJ. 1971. Natural plaque on tooth surfaces: a scanning electron microscopy study. Apex 5:93-8.
47. Jones SJ. 1972. A special relationship between spherical and filamentous microorganisms in mature human dental plaque. Arch Oral Biol 17:613-6.
48. Kaufman J, DiRienzo JM. 1989. Isolation of a corncob (coaggregation) receptor polypeptide from *Fusobacterium nucleatum*. Infect Immun 57:331-7.
49. Soding J, Biegert A, Lupas AN. 2005. The HHpred interactive server for protein homology detection and structure prediction. Nucleic Acids Res 33:W244-8.
50. Froeliger EH, Fives-Taylor P. 2001. *Streptococcus parasanguis* fimbria-associated adhesin Fap1 is required for biofilm formation. Infect Immun 69:2512-9.
51. Loukachevitch LV, Bensing BA, Yu H, Zeng J, Chen X, Sullam PM, Iverson TM. 2016. Structures of the *Streptococcus sanguinis* SrpA Binding Region with Human Sialoglycans Suggest Features of the Physiological Ligand. Biochemistry 55:5927-5937.
52. Pyburn TM, Bensing BA, Xiong YQ, Melancon BJ, Tomasiak TM, Ward NJ, Yankovskaya V, Oliver KM, Cecchini G, Sulikowski GA, Tyska MJ, Sullam PM, Iverson TM. 2011. A structural model for binding of the serine-rich repeat adhesin GspB to host carbohydrate receptors. PLoS Pathog 7:e1002112.

53. Bensing BA, Khedri Z, Deng L, Yu H, Prakobphol A, Fisher SJ, Chen X, Iverson TM, Varki A, Sullam PM. 2016. Novel aspects of sialoglycan recognition by the Siglec-like domains of streptococcal SRR glycoproteins. Glycobiology 26:1222-1234.
54. Bensing BA, Loukachevitch LV, McCulloch KM, Yu H, Vann KR, Wawrzak Z, Anderson S, Chen X, Sullam PM, Iverson TM. 2016. Structural Basis for Sialoglycan Binding by the *Streptococcus sanguinis* SrpA Adhesin. J Biol Chem 291:7230-40.
55. Everest-Dass AV, Jin D, Thaysen-Andersen M, Nevalainen H, Kolarich D, Packer NH. 2012. Comparative structural analysis of the glycosylation of salivary and buccal cell proteins: innate protection against infection by *Candida albicans*. Glycobiology 22:1465-1479.
56. Childers SE, Ciufo S, Lovley DR. 2002. *Geobacter metallireducens* accesses insoluble Fe(III) oxide by chemotaxis. Nature 416:767-9.
57. Bensing BA, Li Q, Park D, Lebrilla CB, Sullam PM. 2018. Streptococcal Siglec-like adhesins recognize different subsets of human plasma glycoproteins: implications for infective endocarditis. Glycobiology 28:601-611.
58. Deng L, Bensing BA, Thamadilok S, Yu H, Lau K, Chen X, Ruhl S, Sullam PM, Varki A. 2014. Oral streptococci utilize a Siglec-like domain of serine-rich repeat adhesins to preferentially target platelet sialoglycans in human blood. PLoS Pathog 10:e1004540.
59. Malpede BM, Lin DH, Tolia NH. 2013. Molecular basis for sialic acid-dependent receptor recognition by the *Plasmodium falciparum* invasion protein erythrocyte-binding antigen-140/BAEBL. J Biol Chem 288:12406-15.
60. Moustafa I, Connaris H, Taylor M, Zaitsev V, Wilson JC, Kiefel MJ, von Itzstein M, Taylor G. 2004. Sialic acid recognition by *Vibrio cholerae* neuraminidase. J Biol Chem 279:40819-26.
61. Varghese JN, Colman PM, van Donkelaar A, Blick TJ, Sahasrabudhe A, McKimm-Breschkin JL. 1997. Structural evidence for a second sialic acid binding site in avian influenza virus neuraminidases. Proc Natl Acad Sci U S A 94:11808-12.